VO$_2$: A Novel View from Band Theory

V. Eyert*

Center for Electronic Correlations and Magnetism, Institute of Physics,
University of Augsburg, 86135 Augsburg, Germany
(Dated: January 19, 2013)

New calculations for vanadium dioxide, one of the most controversly discussed materials for decades, reveal that band theory as based on density functional theory is well capable of correctly describing the electronic and magnetic properties of the metallic as well as both the insulating M$_1$ and M$_2$ phases. Considerable progress in the understanding of the physics of VO$_2$ is achieved by the use of the recently developed hybrid functionals, which include part of the electron-electron interaction exactly and thereby improve on the weaknesses of semilocal exchange functionals as provided by the local density and generalized gradient approximations. Much better agreement with photoemission data as compared to previous calculations is found and a consistent description of the rutile-type early transition-metal dioxides is achieved.

The metal-insulator transition (MIT) of stoichiometric VO$_2$ at ambient pressure [1] has been a matter of ongoing controversy for decades. The issue attained its fundamental character from the discovery of a structural distortion occurring at the same temperature (340 K) as the MIT [2, 3]. Since then, discussion has focused on resolving the hen-and-egg problem of identifying the driving force of the combined electronic-structural transition. The latter is from the high-temperature rutile phase to the low-temperature monoclinic, so-called M$_1$ phase. The distortions occurring at the transition are characterized by metal dimerization parallel to the rutile c axis and a zigzag-like antiferroelectric shift of the V atoms perpendicular to this axis out of the center of the surrounding O octahedra. In a simple molecular-orbital picture these structural changes affect mainly the V $3d$ t_{2g}-derived states, which in the rutile phase straddle the Fermi energy and have similar band occupations [3, 4]. Yet, due to the peculiarities of this structure with its characteristic octahedral chains parallel to the c axis, the t_{2g} states naturally fall into the $d_\parallel$ orbitals and the so-called π^* orbitals, which show a quasi-onedimensional and rather threedimensional dispersion, respectively [5]. Response to the structural changes occurring at the transition to the M$_1$ phase is diverse. While the $d_\parallel$ bands split into occupied bonding and empty antibonding states, the π^* states experience energetical upshift leading to their depopulation [3, 4]. As a consequence, a bandgap opens between the bonding $d_\parallel$ and the π^* bands. An alternative interpretation, emphasizing the electronic origin of the MIT, assigns the splitting of the $d_\parallel$ bands in the insulating phase rather to strong electronic correlations, which are screened by the π^* electrons in the metallic phase [6].

Still, the matter was complicated by the discovery of two additional insulating phases, namely the monoclinic M$_2$ and the triclinic T phase occurring in doped samples or under uniaxial pressure, which suppresses the zigzag-like shift in half of the octahedral chains [7]. In the M$_2$ phase, these chains still show metal dimerization, while in the remaining chains the dimerization is lost in favor of quasi-onedimensional antiferromagnetic ordering. The T phase is intermediate between the two monoclinic phases as, compared to the M$_2$ phase, the dimerized chains start to zigzag and the zigzag chains start to dimerize until both chains are identical and the M$_1$ phase is entered. Of course, the observation of the M$_2$ phase reinitiated the debate about the driving force of the phase transitions and questioned especially the interpretation in terms of particular structural changes underlying the molecular orbital picture.

A somewhat related but more academic aspect of the debate is the question as to what extent band theory would be able to correctly describe and understand the MIT and the role of electronic correlations. This discussion has its roots in the spectacular failure of calculations based on density functional theory (DFT) within the local density (LDA) or generalized gradient approximation (GGA) to reproduce a finite band gap in the single-particle spectrum obtained from the monoclinic structures [5, 8]. Furthermore, from the existence of the $S = \frac{1}{2}$-Heisenberg chains characterizing the M$_2$ phase as well as the fact that, due to simple electrostatic arguments connecting the pairing on one chain to the antiferroelectric shift on the neighboring chains, the M$_1$ and T phases may be regarded as superpositions of two M$_2$-type distortion patterns with equal and unequal amplitude, respectively, Rice *et al.* concluded, that all insulating phases of VO$_2$ must be of the Mott-Hubbard type and are not accessible by band theory [9]. Indeed, LDA calculations for the M$_2$ phase, while leading to an antiferromagnetic ground state, missed the insulating gap like for the M$_1$ phase [5]. This failure could be cured by LDA+U calculations, which, however, resulted in antiferromagnetic insulating ground states also for the M$_1$ and the metallic rutile phase [10]. So far, these latter

two phases could be correctly reproduced only by GW calculations and combinations of LDA with the dynamic mean-field theory [11–14]. Nevertheless, a correct consistent description of the metallic rutile as well as both insulating monoclinic phases using a parameter-free methodology has not yet emerged.

Here, the results of renewed calculations as based on DFT are presented. In contrast to previous work the present investigation builds on the use of the recently developed class of hybrid functionals, which have already proven to allow for a strikingly improved description of semiconductors and insulators [15, 16]. Yet, applications of these new tools to materials, which are regarded as strongly correlated, are still rare due to the high computational demand [15]. The present work demonstrates that density functional theory in combination with hybrid functionals is well capable to generate an insulating gap in the single-particle spectrum of both the M_1 and M_2 phases and to properly describe the antiferromagnetic ordering on the Heisenberg chains of the latter. These results shed new light onto the discussion of the role of the relevant correlations, since hybrid functionals primarily aim at improving on the exchange part of the LDA/GGA, while leaving the correlation functional unaltered.

The calculations were performed using density functional theory as implemented in the ab-initio total-energy and molecular-dynamics program VASP (Vienna ab-initio simulation program) developed at the Universität Wien [17]. The exchange-correlation functional was considered at the level of the generalized gradient approximation (GGA) [18]. In addition, calculations as based on the recently developed hybrid functonals were performed. Within the framework of the generalized Kohn-Sham scheme [19] these functionals combine the exchange functional as arising from the local density approximation (LDA) with the non-local Hartree-Fock expression. In the present work, the functional proposed by Heyd, Scuseria, and Ernzerhof (HSE) was used [20]. In this approach, the short-range part of the exchange functional is represented by a (fixed) combination of GGA- and Hartree-Fock contributions, while the long-range part and the correlation functional are described by the GGA only. The single-particle equations were solved using the projector-augmented wave (PAW) method [21, 22] with a plane-wave basis with a cutoff of 400 eV.

In a first step, the metallic rutile phase was considered. Structural data were taken from the work of McWhan et al. [23] in order to be consistent with previous calculations [5]. Partial densities of states as emerging from spin-degenerate calculations are displayed in Fig. 1. Two groups of bands are recognized. While the fully occupied bands derive mainly from the O $2p$ states, the group of bands straddling the Fermi energy are dominated by the V $3d$ states. V $3d$- and O $2p$-contributions showing up in the energy range, where the respective other orbitals dominate, result from hybridization between these states.
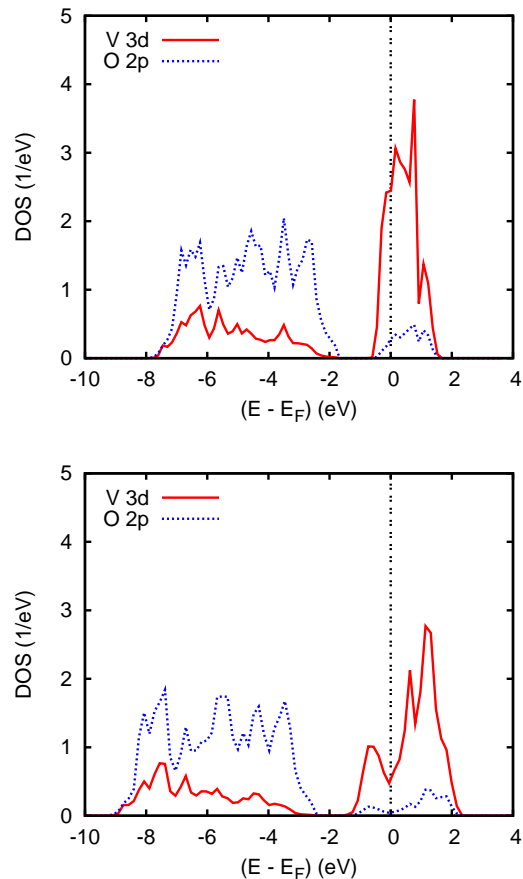

FIG. 1: (Color online) Partial DOS of rutile VO_2 as calculated using the GGA (top) and the HSE (bottom) functional.

The nearly perfect octahedral crystal field splits the V $3d$ levels into weakly π-bonding t_{2g} states ranging from -0.8 to $+1.8$ eV and strong σ-bonding e_g bands, which are found at higher energies but not shown here. The GGA results as displayed in the upper panel of Fig. 1 are very similar to the partial densities of states as arising from previous LDA calculations [5, 8].

The HSE results given in the lower panel of Fig. 1 deviate substantially from those obtained by the GGA. While retaining their shape, the O $2p$ partial densities of states experience 10% broadening and energetical downshift by about 1 eV. In contrast, the width of the V $3d$ states almost doubles leading to an occupied band width of about 1.5 eV and a pronounced peak near -0.75 eV in much better agreement with experiment than the GGA results. In particular, photoemission finds an occupied band width of about 1.5 eV for the V $3d$ band centered at about -1 eV [24, 25].

For the monoclinic M_1 phase, crystal structure data by Longo and Kierkegaard were used [26]. Partial densities of states as arising from GGA calculations are shown in the upper panel of Fig. 2. As for the rutile structure,
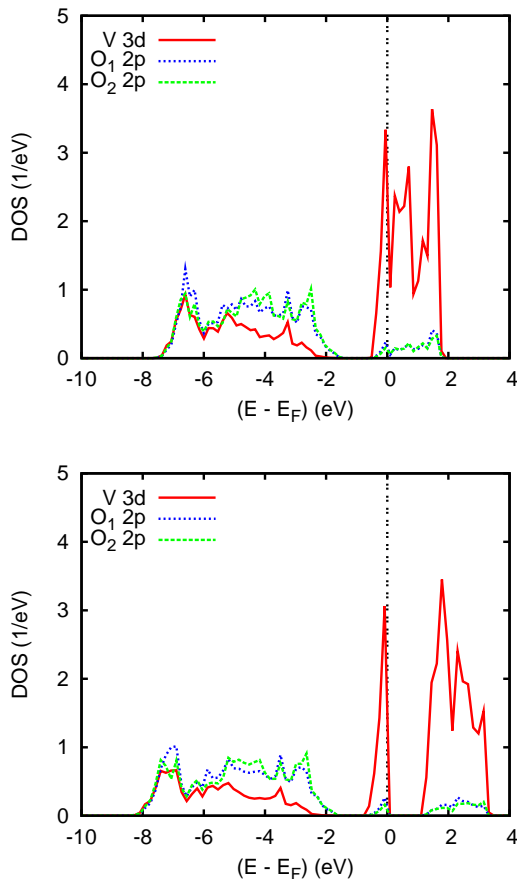
3

FIG. 2: (Color online) Partial DOS of M_1-VO_2 as calculated using the GGA (top) and the HSE (bottom) functional.

FIG. 3: (Color online) Electronic bands of M_1-VO_2 as calculated using the GGA (top) and the HSE (bottom) functional.

these results closely resemble those of previous calculations [5, 8]. Again, the bands fall into O $2p$ and V $3d$ dominated groups well below and at the Fermi energy. Although the V $3d$ states display a sharp dip at E_F, the calculations still reflect the above mentioned failure of LDA/GGA to reproduce the insulating band gap of the monoclinic phase. According to the band structure displayed in the upper panel of Fig. 3 the metallic behaviour results from small semimetallic-like overlap of the characteristic double band ranging from -0.5 eV to slightly above the Fermi energy with the almost empty higher lying bands. Yet, as has been discussed in detail previously, strong orbital ordering is obtained, since the occupied double band derives mainly from the $d_\parallel$ states, whereas the π^* states are found mostly above E_F [5]. This is in striking contrast to the rutile phase, where LDA calculations yield very similar occupations of the t_{2g} bands with only small hybridization between the $d_\parallel$ and π^* states [5]. Thus, the MIT is accompanied by strong orbital switching, as has been confirmed by most calculations as well as by recent XAS measurements [27].
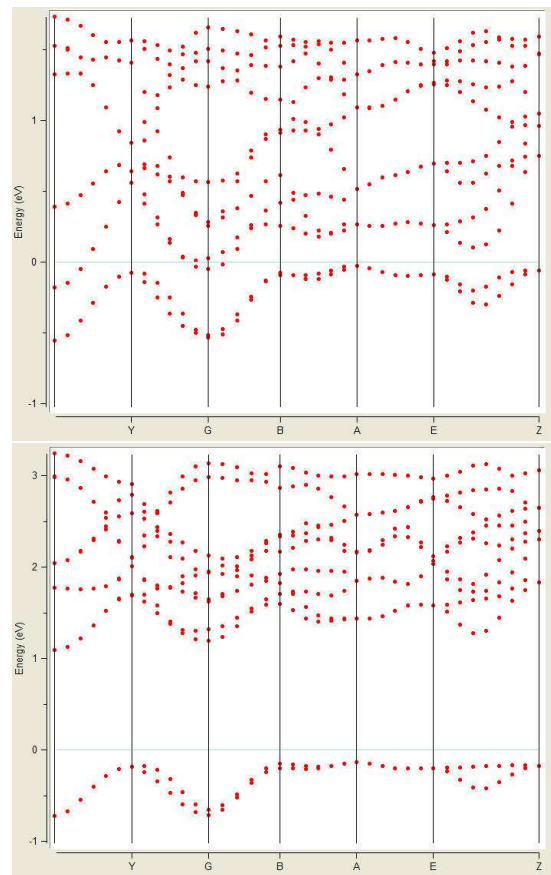
The situation changes drastically on turning to the hybrid functional calculations. According to the partial densities of states displayed in the lower panel of Fig. 2, the previously slightly overlapping groups of bands are pulled apart and an insulating band gap of ≈ 1.1 eV is opened between the bonding $d_\parallel$ bands and the empty π^* states. The bonding $d_\parallel$ bands form a sharp peak at about 0.75 eV below the center of the gap, again in good agreement with photoemission experiments, which find the V $3d$ band of about 1 eV width at a binding energy of about 1 eV [24, 25, 28]. The band structure shown in the lower panel of Fig. 3 reveals a clear separation into fully occupied and empty bands. Furthermore, we note the striking similarity to the GGA bands as concerns both widths and shapes, the main difference being the rather rigid band shift.

Finally, spin-polarized antiferromagnetic calculations were performed for the M_2 phase. Here, crystal structure data as given by Marezio et al. were used [7]. While previous LDA calculations resulted in a stable antiferromagnetic ground state with local magnetic moments of $\approx 0.5\mu_B$ mainly carried by the V $3d$ $d_\parallel$ states, the insulating behaviour could not be reproduced [5]. In contrast, the present HSE calculations lead to V magnetic moments of $1.0\mu_B$ and an optical band gap of about 1.2 eV.
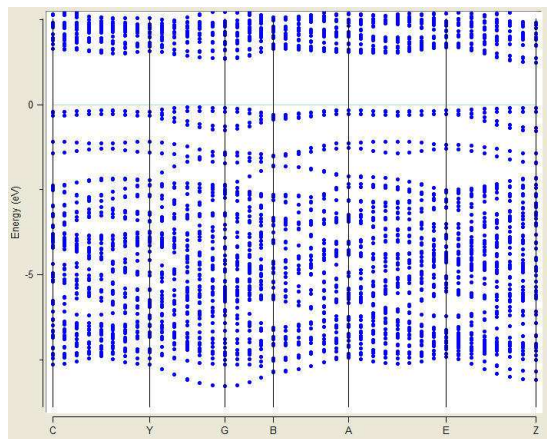
FIG. 4: (Color online) Electronic bands of M_2-VO_2 as calculated using the HSE functional.

This is easily seen in the band structure shown in Fig. 4. Analysis of the corresponding partial densities of states reveals strong polarization of the vanadium atoms in the antiferroelectrically distorted chains, whereas polarization of the dimerizing vanadium atoms is almost negligible.

To conclude, band theory as based on density functional theory is well capable of correctly describing the metal-insulator transitions of VO_2 provided that the appropriate exchange-correlation functional is used. In particular, while LDA and GGA fail to account for the insulating behaviour of the low-temperature phases, the recently proposed hybrid functionals lead to a finite band gap for both the M_1 and M_2 phases and the antiferromagnetic ordering observed for the latter. In addition, much better agreement with photoemission data has been found. Our results put VO_2 in line with the metal-insulator system NbO_2 and metallic MoO_2, which both display the same structural distortions and have already been successfully described within density functional theory [29–31]. We are not aware of any other theory, which has provided a consistent and successful description of the structural distortions of the rutile-type early transition-metal dioxides as well as the MIT's of the d^1 members. Finally, the present study sheds new light on the old discussion about the predominant influence of either structural distortions or electronic correlations as no further interactions beyond those covered by density functional theory and the Hartree-Fock exchange have to be introduced. However, recent experimental studies indicate that the insulator-to-metal transition is initiated by rearrangements of the electronic system [32, 33]. A theoretical understanding of these data is the subject of current research.

* Present address: Materials Design, 92120 Montrouge, France; Email: veyert@materialsdesign.com
[1] F. J. Morin, Phys. Rev. Lett. **3**, 34 (1959).
[2] G. Andersson, Acta Chim. Scand. **8**, 1599 (1954); **10**, 623 (1956).
[3] J. B. Goodenough, Phys. Rev. **117**, 1442 (1960).
[4] J. B. Goodenough, J. Solid State Chem. **3**, 490 (1971).
[5] V. Eyert, Ann. Phys. (Leipzig) **11**, 650 (2002).
[6] A. Zylbersztejn and N. F. Mott, Phys. Rev. B **11**, 4383 (1975).
[7] M. Marezio, D. B. McWhan, J. P. Remeika, and P. D. Dernier, Phys. Rev. B **5** (1972) 2541.
[8] R. M. Wentzcovitch, W. W. Schulz, and P. B. Allen, Phys. Rev. Lett. **72**, 3389 (1994); **73**, 3043 (1994).
[9] T. M. Rice, H. Launois, and J. P. Pouget, Phys. Rev. Lett. **73**, 3042 (1994).
[10] M. A. Korotin, N. A. Shorikov, and V. I. Anisimov, Phys. Met. Metallogr. **94**, 17 (2002).
[11] A. Continenza, S. Massidda, and M. Posternak, Phys. Rev. B **60**, 15699 (1999).
[12] M. Gatti, F. Bruneval, V. Olevano, and L. Reining, Phys. Rev. Lett. **99**, 266402 (2007).
[13] S. Biermann, A. Poteryaev, A. I. Lichtenstein, and A. Georges, Phys. Rev. Lett. **94**, 026404 (2005).
[14] J. M. Tomczak and S. Biermann, J. Phys.: Condens. Matter **19**, 365206 (2007).
[15] M. Marsman, J. Paier, A. Stroppa, and G. Kresse, J. Phys.: Cond. Matt. **20**, 064201 (2008).
[16] T. Shimazaki, and Y. Asai, J. Chem. Phys. **132**, 224105 (2010).
[17] G. Kresse and J. Furthmüller, Phys. Rev. B **54**, 11169 (1996); Comput. Mater. Sci. **6**, 15 (1996).
[18] J. P. Perdew, K. Burke, and M. Ernzerhof, Phys. Rev. Lett. **77**, 3865 (1996).
[19] A. Seidl, A. Görling, P. Vogl, J. A. Majewski, and M. Levy, Phys. Rev. B **53**, 3764 (1996).
[20] J. Heyd, G. E. Scuseria, and M. Ernzerhof, J. Chem. Phys. **118**, 8207 (2003), J. Chem. Phys. **124**, 219906 (2006).
[21] G. Kresse and D. Joubert, Phys. Rev. **59**, 1758 (1999).
[22] P. E. Blöchl, Phys. Rev. **50**, 17953 (1994).
[23] D. B. McWhan, M. Marezio, J. P. Remeika, and P. D. Dernier, Phys. Rev. B **10**, 490 (1974).
[24] S. Shin, S. Suga, M. Taniguchi, M. Fujisawa, H. Kanzaki, A. Fujimori, H. Daimon, Y. Ueda, K. Kosuge, and S. Kachi, Phys. Rev. B **41** (1990) 4993.
[25] K. Okazaki, H. Wadati, A. Fujimori, M. Onoda, Y. Muraoka, and Z. Hiroi, Phys. Rev. B **69**, 165104 (2004).
[26] J. M. Longo and P. Kierkegaard, Acta Chim. Scand. **24** (1970) 420.
[27] M. W. Haverkort, Z. Hu, A. Tanaka, W. Reichelt, S. V. Streltsov, M. A. Korotin, V. I. Anisimov, H. H. Hsieh, H.-J. Lin, C. T. Chen, D. I. Khomskii, and L. H. Tjeng, Phys. Rev. Lett. **95**, 196404 (2005).
[28] T. C. Koethe, Z. Hu, M. W. Haverkort, C. Schüßler-

Langeheine, F. Venturini, N. B. Brookes, O. Tjernberg, W. Reichelt, H. H. Hsieh, H.-J. Lin, C. T. Chen, and L. H. Tjeng, Phys. Rev. Lett. **97**, 116402 (2006).

[29] V. Eyert, Europhys. Lett. **58**, 851 (2002).

[30] V. Eyert, R. Horny, K.-H. Höck, and S. Horn, J. Phys.: Condens. Matter **12**, 4923 (2000).

[31] J. Moosburger-Will, J. Kündel, M. Klemm, S. Horn, P. Hofmann, U. Schwingenschlögl, and V. Eyert, Phys. Rev. B **79**, 115113 (2009).

[32] J. Cao, W. Fan, K. Chen, N. Tamura, M. Kunz, V. Eyert, and J. Wu, Phys. Rev. B **82**, 241101(R) (2010).

[33] H. Dachraoui, G. Obermeier, C. Oberer, N. Müller, S. Horn, V. Eyert, and U. Heinzmann, preprint.